Cell Death and Differentiation (2014) 21, 612–623

www.nature.com/cdd

OPEN

ROS-dependent activation of JNK converts p53 into an efficient inhibitor of oncogenes leading to robust apoptosis

Y Shi[1], F Nikulenkov[1], J Zawacka-Pankau[1,2], H Li[1], R Gabdoulline[3,5], J Xu[4], S Eriksson[4], E Hedström[1,6], N Issaeva[1,7], A Kel[3,8], ESJ Arnér[4] and G Selivanova*[,1]

Rescue of the p53 tumor suppressor is an attractive cancer therapy approach. However, pharmacologically activated p53 can induce diverse responses ranging from cell death to growth arrest and DNA repair, which limits the efficient application of p53-reactivating drugs in clinic. Elucidation of the molecular mechanisms defining the biological outcome upon p53 activation remains a grand challenge in the p53 field. Here, we report that concurrent pharmacological activation of p53 and inhibition of thioredoxin reductase followed by generation of reactive oxygen species (ROS), result in the synthetic lethality in cancer cells. ROS promote the activation of c-Jun N-terminal kinase (JNK) and DNA damage response, which establishes a positive feedback loop with p53. This converts the p53-induced growth arrest/senescence to apoptosis. We identified several survival oncogenes inhibited by p53 in JNK-dependent manner, including Mcl1, PI3K, eIF4E, as well as p53 inhibitors Wip1 and MdmX. Further, we show that Wip1 is one of the crucial executors downstream of JNK whose ablation confers the enhanced and sustained p53 transcriptional response contributing to cell death. Our study provides novel insights for manipulating p53 response in a controlled way. Further, our results may enable new pharmacological strategy to exploit abnormally high ROS level, often linked with higher aggressiveness in cancer, to selectively kill cancer cells upon pharmacological reactivation of p53.
Cell Death and Differentiation (2014) **21,** 612–623; doi:10.1038/cdd.2013.186; published online 10 January 2014

The p53 tumor suppressor is a promising target for cancer therapy; several compounds targeting p53 are currently being tested in clinical setting.[1] *In vivo* studies support the idea of pharmacological restoration of p53 to combat cancer.[2–4] Activation of p53 can lead to growth arrest, senescence or cell death, but elucidation of the molecular mechanisms driving the life/death decision by p53 remains one of the grand challenges in p53 biology.[5] As the p53-mediated senescence or growth arrest can prevent cancer cell killing by chemotherapy thus leading to poor clinical outcome,[6] it is imperative to understand the mechanism of p53-mediated cell fate decisions for the efficient clinical application of drugs activating p53.

We have previously shown that in spite of different transcriptional programs induced by p53 in breast cancer cells upon administration of different p53-activating compounds, p53 binds the same set of genes, irrespective of the type of treatment.[7] This finding supports the view that the heterogeneous response and selective regulation of p53 target genes is likely to be influenced by other signal transduction pathways. A wealth of studies have looked into the p53 interactions with its partners and the type of p53 posttranslational modifications, but it still remains elusive, when, how and which factors direct p53 to a certain transcriptional program.[5] A number of p53-modifying enzymes have been identified, including checkpoint kinases ATM/ATR, Chk2,[5] as well as mitogen-activated protein kinases (MAPK) p38 and c-Jun N-terminal kinase JNK[8] induced by oxidative stress.

Cancer cells frequently have increased burden of oxidative stress[9] and therefore are likely to be more sensitive to the damage promoted by further reactive oxygen species (ROS) insults. Recent studies have revealed the dependency of cancers on redox-regulating mechanisms, such as the glutaredoxin and the thioredoxin systems, to be the cancer-specific vulnerability thereby offering a target for treatment of malignancies.[9,10] The NADPH-dependent selenoprotein thioredoxin reductase (TrxR), often overexpressed in cancer,

[1]Department of Microbiology, Tumor and Cell Biology (MTC), Karolinska Institutet 17177, Stockholm, Sweden; [2]Department of Biotechnology, Intercollegiate Faculty of Biotechnology, UG-MUG 80-822, Gdansk, Poland; [3]geneXplain GmbH D-38302, Wolfenbüttel, Germany and [4]Division of Biochemistry, Department of Medical Biochemistry and Biophysics, Karolinska Institutet, Stockholm, Sweden
*Corresponding author: G Selivanova, Department of Microbiology, Tumor and Cell Biology (MTC), Karolinska Institutet, Nobelsväg 16, Box 280, Stockholm 17177, Sweden. Tel: +46 8 524863 02; Fax: +46 8 342651; E-mail: galina.selivanova@ki.se
[5]Current address: Heinrich-Heine University of Duesseldorf, Universitaetstr. 1, 40225, Duesseldorf.
[6]Current address: Cancer Center Karolinska, Karolinska Institutet, Stockholm, Sweden.
[7]Current address: Division of Otolaryngology, Yale School of Medicine, P.O. Box 208062, New Haven, CT 06520-8062, USA.
[8]Current address: Institute of Chemical Biology and Fundamental Medicine, SBRAS, Lavrentyeva St. 8, 630090 Novosibirsk, Russia.
Keywords: TrxR; ROS; JNK; p53; Wip1; inhibition of oncogenes
Abbreviations: ROS, reactive oxygen species; JNK, c-Jun N-terminal kinase; TrxR, thioredoxin reductase; DDR, DNA damage response; PFTα, pifithrin-α; Nut, nutlin; Aura, auranofin; NAC, N-Acetyl-L-cysteine; NDGA, nordihydroguaiaretic acid; CDDP, cisplatin; NCS, neocarzinostatin; DCF-DA, 2′,7′-dichlorodihydrofluorescein diacetate; FACS, fluorescence-activated cell sorting; ChIP-seq, chromatin immunoprecipitation followed by deep sequencing
Received 28.6.13; revised 04.10.13; accepted 20.11.13; Edited by K Vousden; published online 10.1.14

is one of the promising anti-cancer drug targets, which is inhibited by several anti-cancer drugs in clinical use.[11,12]

In the present study, we identified ROS-activated JNK as a crucial p53 co-regulator, revealing a strategy to switch the p53 transcriptional response from growth arrest to apoptosis upon its pharmacological activation.

Results

Transient *versus* sustained changes in gene expression upon p53-mediated growth arrest and apoptosis. To address the mechanisms of the differential biological outcome upon p53 activation, we used as molecular probes p53-reactivating molecules RITA and nutlin (Nut), which inhibit p53/MDM2 interaction.[13] As a model, we applied a pair of cell lines, breast carcinoma MCF7 and colon carcinoma HCT116, in which activation of p53 by 10 μM Nut and 0.1 μM RITA leads to growth inhibition, whereas 1 μM RITA induces apoptosis.[14,15] As high doses of Nut induce p53-independent cell death (Supplementary Figure S1C), we used 10 μM Nut, inducing p53-dependent response.

We compared the kinetics of gene expression changes in MCF7 cells upon treatment with 10 μM Nut, 0.1 or 1 μM RITA at 10 time points using microarray analysis. Systematic clustering analysis showed that the genes involved in cell cycle regulation, metabolic and biosynthetic processes were continuously repressed upon 1 μM RITA; in contrast, these genes were only transiently repressed after Nut and 0.1 μM RITA treatment (clusters 0001 and 0002 in Figure 1a and Supplementary Table S1).

Another gene cluster, comprising the stress response genes, was continuously induced by 1 μM RITA, but only

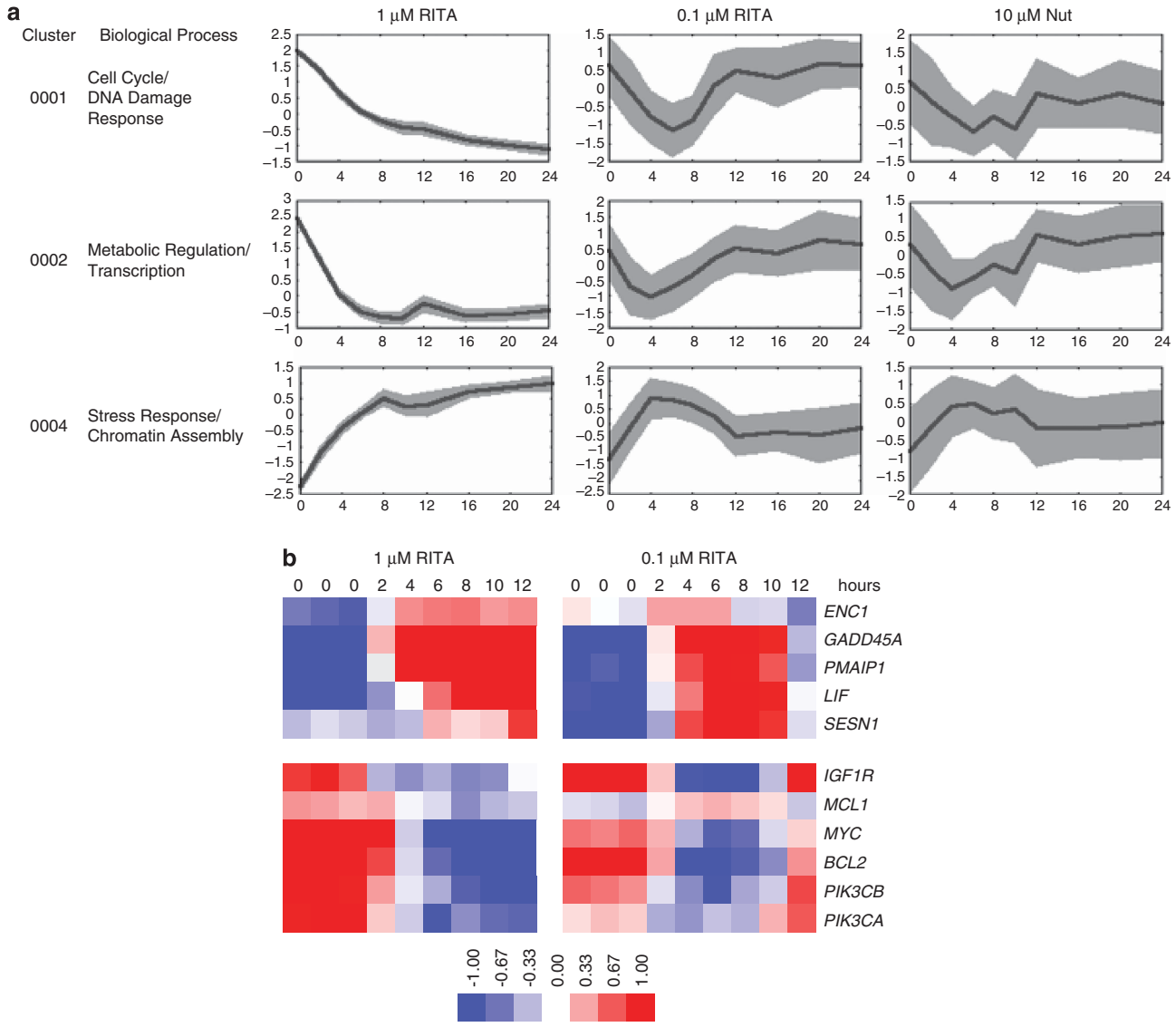

Figure 1 Different kinetics of gene expression upon pharmacologically activated p53. (**a**) Systematic clustering analysis of gene expression profiles revealed distinct kinetics of transcription of several gene clusters upon treatment with different doses of RITA or Nut for 0, 2, 4, 6, 8, 10, 12, 16, 20, 24 h in MCF7 cells. The plots show mean profile (bold) and RMS deviation (gray) for genes, found to have clustered profiles upon 1 μM RITA. (**b**) Heatmaps of representative p53 target genes differentially regulated by 0.1 and 1 μM RITA in MCF7 cells. Values are normalized to untreated control

transiently upregulated by Nut and 0.1 μM RITA (cluster 0004 in Figure 1a).

Next, we analyzed whether known p53 target genes are regulated in a similar differential manner. We found that 1 μM RITA led to the sustained induction of *ENC1, GADD45A, PMAIP1, LIF* and *SESN1,* and inhibition of pro-survival genes *IGF-1R, MCL1, MYC, BCL2, PIK3CA* and *PIK3CB*; however, changes in the expression of these genes were only transient upon 0.1 μM RITA (Figure 1b).

In conclusion, the induction of apoptosis was associated with the sustained p53-mediated transcriptional response. This prompted us to investigate the factors underlying this phenomenon.

ATM-independent induction of p53-dependent DDR upon 1 μM RITA. In line with the previous findings,[16] we observed an increased phosphorylation of H2AX on Ser139 (γH2AX), a hallmark of DNA damage response (DDR), and phosphorylation of p53 on Ser15 (p-S15-p53) upon 1 μM RITA in a time-dependent manner in MCF7, HCT116 (Figure 2a) and U2OS cells (Supplementary Figure S1A). In contrast, low dose of RITA only barely affected the DDR (Figures 2a, 4a and 5b and Supplementary Figure S1A), as did Nut,[17] which correlates with the inefficient apoptosis induction, as evidenced by cleaved PARP levels (Figure 4a and Enge *et al.*[14] and Grinkevich *et al.*[15]).

Importantly, the induction of γH2AX by RITA was observed only in the presence of p53, that is, in the p53-positive HCT116 cells, but not in the p53-null HCT116 p53 $-/-$, osteosarcoma Saos2 and lung adenocarcinoma H1299 cells (Figure 2c, left and right panel). The p53 dependence of γH2AX induction was further supported by the ablation of

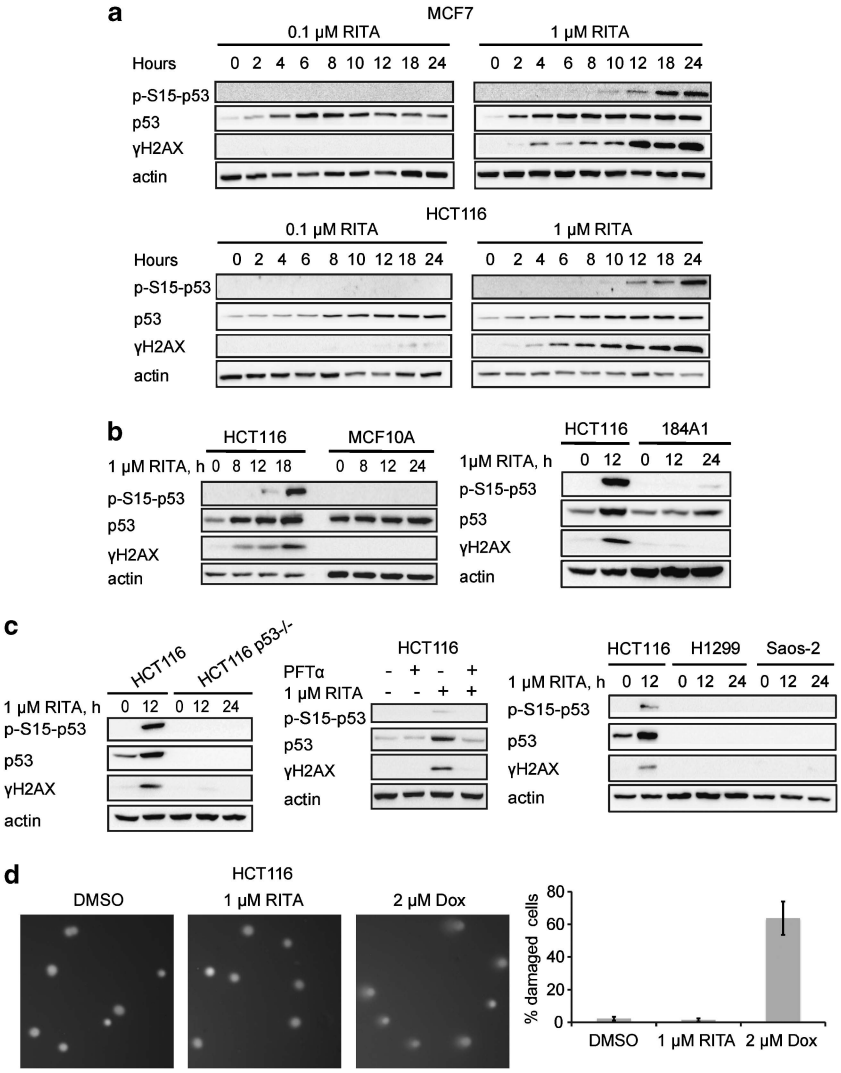

Figure 2 p53- and dose-dependent induction of DDR by RITA in cancer cells, but not in non-tumorigenic cells. (**a**) MCF7 and HCT116 cells were treated with 0.1 and 1 μM RITA for indicated periods and levels of p53, γH2AX and p-S15-p53 were detected by immunoblotting. Actin was used as a loading control. (**b**) RITA did not induce γH2AX in non-tumorigenic MCF10A and 184A1 cells as assessed by immunoblotting. (**c**) Wild-type p53-expressing cells HCT116 and p53-null HCT116 p53 $-/-$, H1299, Saos2 cells were treated with 1 μM RITA for indicated periods (upper and lower panels); HCT116 cells were pretreated with pifithrin-α for 2 h and treated with 1 μM RITA for 12 h (middle panel). Proteins were analyzed by western blotting. (**d**) HCT116 cells were treated with 1 μM RITA or doxorubicin for 12 h and DNA strand breaks were assessed by comet assay. Right panel, quantification of cells containing strand breaks (mean $\pm$ S.E.M., $n=3$)

γH2AX by the p53 inhibitor pifithrin-α (PFTα)[18] and upon p53 depletion with siRNA (Figure 2c, middle panel and Supplementary Figure S1B, respectively). We ruled out the possibility that DDR was induced upon DNA fragmentation during apoptosis, as the pretreatment with a pan-caspase inhibitor Z-VAD-fmk did not prevent γH2AX, whereas it did prevent PARP cleavage (Supplementary Figure S1D).

Alkaline comet assay revealed that a 'comet tail', indicating DNA strand breaks, was barely detectable upon 1 μM RITA, whereas positive control doxorubicin produced a clear pattern (Figure 2d). We did not detect DNA strand breaks using pulse-field electrophoresis assay either (Supplementary Figure S1E). Thus, in line with the previously published data,[16,19] RITA produces a low number of strand breaks, if any. Importantly, RITA did not induce the DDR and apoptosis in the non-tumorigenic cells MCF10A and 184A1 (Figure 2b and Supplementary Figure S2F).

To find out the mechanism of DDR induction, we tested the involvement of checkpoint kinases. Depletion of ATM by siRNA did not prevent γH2AX and p53 accumulation, neither did the pretreatment with the ATM inhibitor KU55933 or with the major DDR kinase inhibitor caffeine (Supplementary Figures S1F–H), ruling out the involvement of these kinases. However, the kinetics and the extent of p53 accumulation were partially affected by caffeine (Supplementary Figure S1H), suggesting that DDR contributes to the faster and robust induction of p53, perhaps via amplification of the signaling to p53.

In conclusion, the induction of DDR was p53-, but not ATM/ATR-dependent and correlated with the induction of apoptosis.

Generation of ROS leads to DDR and confers synthetic lethality upon p53 reactivation. Since ROS can cause DDR,[20] we reasoned that the induction of γH2AX could be due to the p53-dependent induction of ROS resulting from the inhibition of TrxR1 by 1 μM RITA, reported previously by us.[21] More detailed analysis of the effect of RITA on TrxR1 in *in vitro* enzymatic assay revealed that while RITA inhibited the reducing activity of TrxR1 on two different substrates, it barely affected its NADPH oxidase function (Figure 3a), which endows the enzyme with pro-oxidant activity.[22,23] Thus, both the inhibited reductase and the sustained oxidase activities of TrxR1 upon RITA should contribute to ROS accumulation. Indeed, 1 μM RITA induced intracellular ROS in MCF7 and HCT116 cells, whereas a low dose of RITA or Nut did not trigger ROS (Figure 3b, Supplementary Figures S2A, S3A and B). In line with our previously published results,[21] ROS were not induced in non-transformed MCF10A cells (Supplementary Figures S2E and S3C), correlating with the absence of DDR. Thus, DDR was associated with the induction of ROS.

Next, we addressed the question whether generation of ROS is the cause of DDR and whether it contributes to p53-mediated cell death. We found that ROS scavenger *N*-Acetyl-L-cysteine (NAC), as well as a low dose (1 μM) of antioxidant resveratrol[24] inhibited ROS induced by RITA (Figure 3c, Supplementary Figures S2B, S3A and B). Notably, both antioxidants prevented the induction of γH2AX (Figure 3d and Supplementary Figure S2C), supporting our idea that the induction of DDR is triggered by ROS.

However, NAC or resveratrol did not prevent the accumulation of p53 by RITA, indicating that p53 induction is not due to ROS.

NAC and resveratrol partially reversed the apoptosis triggered by RITA, as evidenced by the decreased PARP cleavage and the rescue of cell viability (Figure 3d and Supplementary Figures S2C and S4A). These data corroborated the involvement of ROS in p53-mediated apoptosis. Accordingly, fluorescence-activated cell sorting (FACS) analysis of propidium iodide (PI) stained cells confirmed that resveratrol, as well as another potent antioxidant nordihydroguaiaretic acid (NDGA)[25] significantly inhibited apoptosis upon RITA (Supplementary Figure S2D).

To reinforce the role of ROS as a possible denominator of the apoptotic response upon p53 reactivation, we examined whether blocking TrxR by auranofin (Aura), a well-known inhibitor of TrxR[26] and inducer of ROS (Figure 3b and Supplementary Figure S2A), could convert the growth arrest/senescence induced by Nut into apoptosis. As evident from Figure 3e, a low dose of Aura was synthetic lethal with p53 activation by low dose Nut. This is manifested by the robust induction of apoptosis upon Aura/Nut combination, while both agents barely induced cell death, when taken alone; importantly, NAC reverted the synthetic lethality induced by the combination of Nut and Aura (Figures 3e and f, and Supplementary Figure S4C). We also observed a synergistic effect upon the combination of low dose of RITA and Aura; similarly, NAC reverted the synthetic lethality upon low dose of RITA and Aura as well (Figures 3f and g and Supplementary Figure S4C).

To elucidate whether ROS contribute to the apoptosis induction upon other types of pharmacological activation of p53, we used cisplatin (CDDP), which has been shown to activate p53 and inhibit the TrxR enzyme activity.[27,28] We found that pretreatment with NAC, resveratrol or NDGA prevented the elimination of tumor cells by CDDP (Supplementary Figure S4B).

Taken together, our data suggest that disabling the oxidative defense mechanisms in cancer cells, for instance, via TrxR inhibition, is synthetic lethal when combined with the pharmacological restoration of p53.

Activation of JNK triggered by ROS mediates the synthetic lethality upon p53 activation and inhibition of TrxR. Next, we investigated which factor mediates the synthetic lethal effect of p53 activation combined with TrxR inhibition. The activation of MAP kinase JNK upon inhibition of TrxR[29] and its ability to modulate p53 make JNK an attractive candidate mediator of ROS signaling to p53. We found that RITA induced JNK phosphorylation (p-JNK) in a p53- and dose-dependent manner (Figures 4a and b). Notably, the induction of p-JNK was conferred by the increased ROS levels, as NAC and resveratrol inhibited JNK activation (Figure 4c and Supplementary Figure S5A). Importantly, JNK serves as a critical mediator of the p53-induced apoptosis, as evidenced by the rescue of PARP cleavage, growth suppression and subG1 fraction by JNK inhibitor SP600125 and siRNA-mediated depletion of JNK (Figures 4d and h and Supplementary Figures S5B and C).

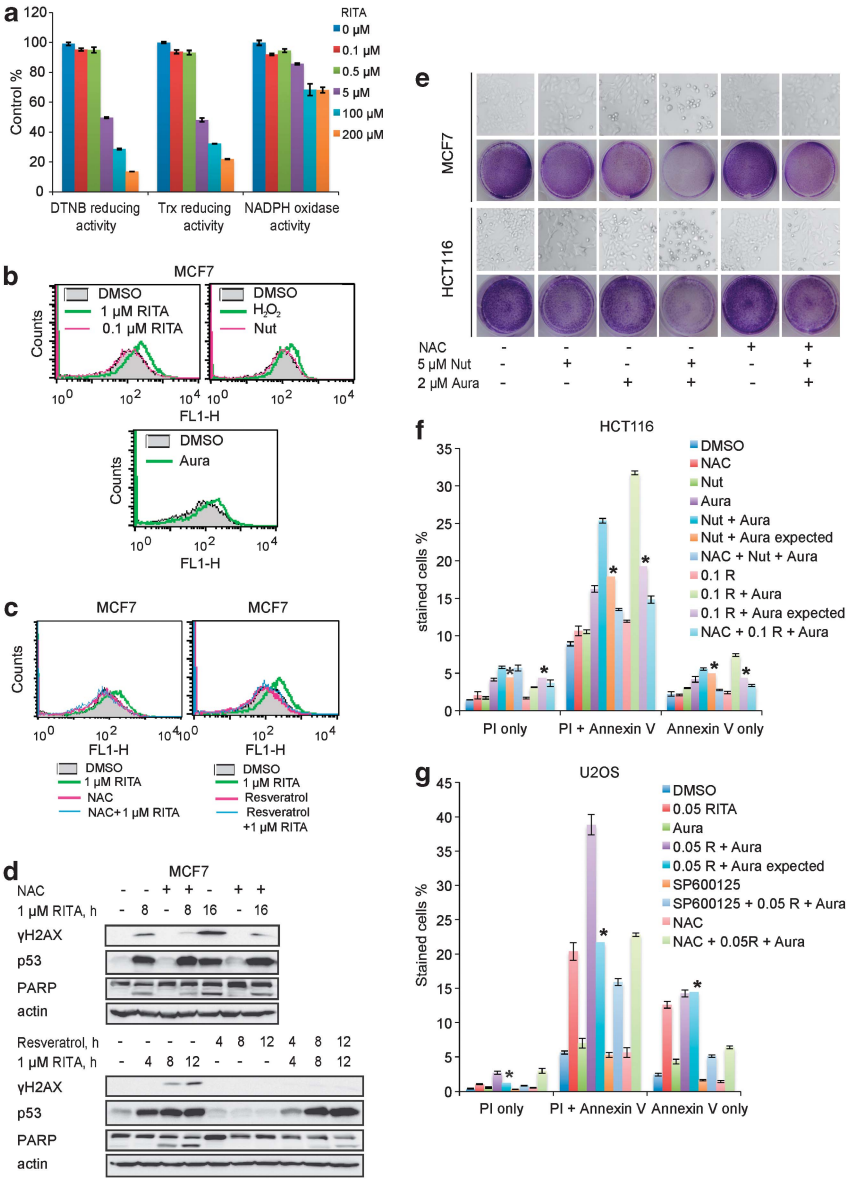

Figure 3 Induction of ROS leads to DDR and p53-dependent apoptosis. (**a**) Dose-dependent inhibition of the ability of TrxR1 to reduce 5,5′-dithiobis (2-nitrobenzoic acid) (DTNB) and thioredoxin (Trx), but not its NADPH oxidase activity by RITA, as measured in *in vitro* assay using purified TrxR1. (**b**) ROS were measured in MCF7 cells treated for 6 h with 0.1 and 1 μM RITA (upper left panel), Nut or 400 μM H_2O_2 (upper right panel) and 5 μM TrxR inhibitor Aura as a positive control (lower panel). (**c**) Antioxidants NAC and resveratrol prevent the induction of ROS by 1 μM RITA. (**d**) Antioxidants NAC (upper panel) and resveratrol (lower panel) inhibited the induction of γH2AX and PARP cleavage by RITA as analyzed by western blotting. (**e**) MCF7 and HCT116 cells were treated with 2 μM Aura or 5 μM Nut, or their combination (with or without NAC pretreatment) for 48 h; cells were photographed before proceeding to crystal violet staining. (**f**) HCT116 cells were treated with 2 μM Aura, 10 μM Nut or 0.1 μM RITA, or their combination (with or without NAC pretreatment) for 48 h; then cells were harvested and proceeded to double staining with Annexin V and propidium iodide (PI) followed by FACS analysis (mean ± S.E.M., $n = 3$). PI only: necrotic and/or late apoptotic cells; PI + Annexin V: apoptotic cells; Annexin V only: early apoptotic cells; *expected additive effect. (**g**) U2OS cells were treated with 1 μM Aura or 0.05 μM RITA, or their combination (with or without NAC or 10 μM SP600125 pretreatment) for 48 h and assessed as in (**f**) (mean ± S.E.M., $n = 3$); *expected additive effect

Furthermore, we found that the synthetic lethal effect of the low dose of RITA/Aura combination is mediated by p-JNK. Aura combined with the low dose of RITA led to the robust induction of p-JNK. Notably, the induction of apoptosis upon this combination treatment, manifested as PARP cleavage, was prevented by JNK inhibitor (Figure 4e).

Thus, we concluded that JNK is a crucial player downstream of ROS in the molecular pathway leading to the synthetic lethality upon p53 activation combined with TrxR inhibition.

JNK activated by ROS contributes to the induction of DDR and converts p53 into an efficient inhibitor of oncogenes. Next, we focused on elucidating the mechanisms by which JNK enhances p53-induced apoptosis. As JNK has been shown to mediate the UV-induced γH2AX,[30]

we assessed the role of JNK in γH2AX accumulation. JNK inhibitor SP600125, as well as JNK depletion by siRNA, markedly reduced γH2AX (Figures 4d and f and Supplementary Figure S5B), implying that JNK is the critical kinase mediating DDR. In addition, JNK mediated p53 phosphorylation at Ser33 (Figures 4d, e and g and Supplementary Figure S5D).

Strikingly, the p53-dependent downregulation of several oncogenes, anti-apoptotic factor Mcl1 and p53 inhibitors Wip1 and MdmX (Figure 4b, Supplementary Figure S1B), was rescued by NAC, resveratrol and JNK inhibitor (Figures 4c and e and Supplementary Figures S5A and B). Further evidence of the crucial role of ROS and JNK in oncogene downregulation by p53 was provided by the experiments in which we used the combination of the low dose of RITA and Aura. Although Wip1 expression was increased upon the low dose of RITA, its induction was partially prevented by Aura (Figure 4e). Moreover, the combination of low dose of RITA and Aura led to a dramatic downregulation of MdmX. Notably, Aura-mediated downregulation of Wip1 and MdmX was rescued by JNK inhibitor (Figure 4e).

The JNK-dependence of Wip1 and MdmX downregulation was further supported by the JNK depletion experiments (Figure 4g and Supplementary Figure S5D).

Interestingly, the p53 level was largely unaffected by the JNK inhibitor, as well as the induction of its target genes Puma and Noxa (Figures 4c and d and Supplementary Figures S5A and B).

Next, we assessed whether the observed inhibition of oncogenes occurs on mRNA level. In line with our previous results,[15] RT-qPCR experiments demonstrated that pharmacological activation of p53 led to a decreased mRNA level of a set of oncogenes, including *MCL1*, Wip1-encoding *PPM1D*, *MDM4* (MdmX), as well as *PIK3CA* and *PIK3CB*, encoding catalytic subunits of PI3 kinase, and translation factor *EIF4E* (Figure 4i). The rescue of oncogene inhibition by JNK inhibitor corroborated the key role of JNK (Figure 4i). In addition, we have previously shown that *MCL1*, *PIK3CA* and *PIK3CB* are not downregulated by the low dose of RITA or nultin; however, their inhibition converts the p53-mediated growth arrest into apoptosis.[15,31]

Therefore, we concluded that the induction of ROS upon RITA leads to the activation of JNK that mediates the phosphorylation of H2AX at Ser139, phosphorylation of p53 at Ser33 and the inhibition of the expression of a set of pro-survival oncogenes by p53, conferring apoptosis induction.

Next, we addressed the question whether and how the repression of *PPM1D*, downstream of JNK, contributes to the synthetic lethal effect.

Inhibition of Wip1 by p53 promotes the induction of γH2AX. p53 activation is opposed by Wip1, an oncogene that removes inactivating phosphorylation marks from Mdm2 and activating phosphorylation marks from p53, $p14/p19^{ARF}$ and checkpoint kinases,[32] and dephosphorylates γH2AX,[33,34] thereby attenuating DDR. Moreover, Wip1 is a p53 target gene that serves as one of the critical determinants of the biological outcome.[34,35] These data and our present results showing that Wip1 activation was induced by Nut and low dose of RITA (Supplementary Figures S6D and E and Figure 4e, respectively), but was repressed by 1 μM RITA in the JNK-dependent manner, prompted us to test how inhibition of Wip1 contributes to p53 activity.

We found that the decline of Wip1 mRNA and protein levels upon RITA strongly correlated with γH2AX induction (Figures 5a and b).

Inhibition of Wip1 has a role in DDR induction upon RITA, as its depletion by shRNA in combination with the low dose of RITA significantly increased the level of γH2AX, comparable with the level induced by 1 μM RITA (Figure 5c).

The negative contribution of Wip1 to DDR was supported by a significantly reduced induction of γH2AX by RITA upon Wip1 overexpression, as assessed by western blotting (Figure 5d).

Wip1 depletion enhances the transactivation function of p53 and contributes to the synthetic lethality. We reasoned that the enhancement of DDR resulting from Wip1 downregulation could facilitate the p53 transcriptional activity leading to a more robust response. To assess this notion, we analyzed the p53 transcriptional response upon Wip1 silencing in MCF7 cells treated with the low dose (0.1 μM) RITA for 4 and 16 h using microarray analysis.

Wip1 depletion *per se* only weakly affected the expression of p53 target genes (Figure 6a). Low dose of RITA induced several p53 targets including *GPRC5A*,[7] *TNFRSF10B* (KILLER/DR5), *FAS*, *RPRM* and *ENC1* (PIG10);[36] however, their induction was not observed at a late time point. Unsupervised clustering analysis indicated similarity of the profiles obtained at 16 h of treatment with control samples (Figure 6a).

Notably, Wip1 depletion by shRNA facilitated the induction of several p53 targets by the low dose of RITA and rescued their decline at 16 h (Figure 6a). This indicates that the inhibition of Wip1 boosts transactivation by p53 and confers its sustainability.

qPCR experiments confirmed that upon Wip1 silencing the expression of p53 targets *FAS*, *GDF15* and *BTG2* was substantially induced, further elevated upon 0.1 μM RITA and lasted longer (Figure 6c, upper panel), confirming that the inhibition of Wip1 leads to an enhanced and sustained p53-mediated transactivation.

However, Wip1 silencing did not facilitate the downregulation of the pro-survival genes (Figures 6b and c, lower panel), which are inhibited by 1 μM RITA in a p53-dependent manner.[15] In line with these data, ectopic expression of Wip1 did not prevent RITA-induced downregulation of Mcl1 (Figure 5d). Further, we found that Wip1 overexpression did not relieve the repression of *PIK3CA, PI3KCB* and *IGF-1R* (Figure 6d). These results suggest that in contrast to p53 transactivation function, p53-mediated inhibition of oncogenes is less tightly regulated by Wip1.

Next, we addressed whether inhibition of Wip1 contributes to the biological response triggered by p53. Indeed, Wip1 depletion promoted the apoptosis induced by both 0.1 and 1 μM RITA, as shown in Figure 6e and Supplementary Figures S6A and B.

As shown in Figure 4e and Supplementary Figure S6E, Aura partially prevented the induction of Wip1 by low RITA or Nut in U2OS cells as well as triggered the downregulation of Mdm2 and MdmX and apoptosis (Supplementary Figures

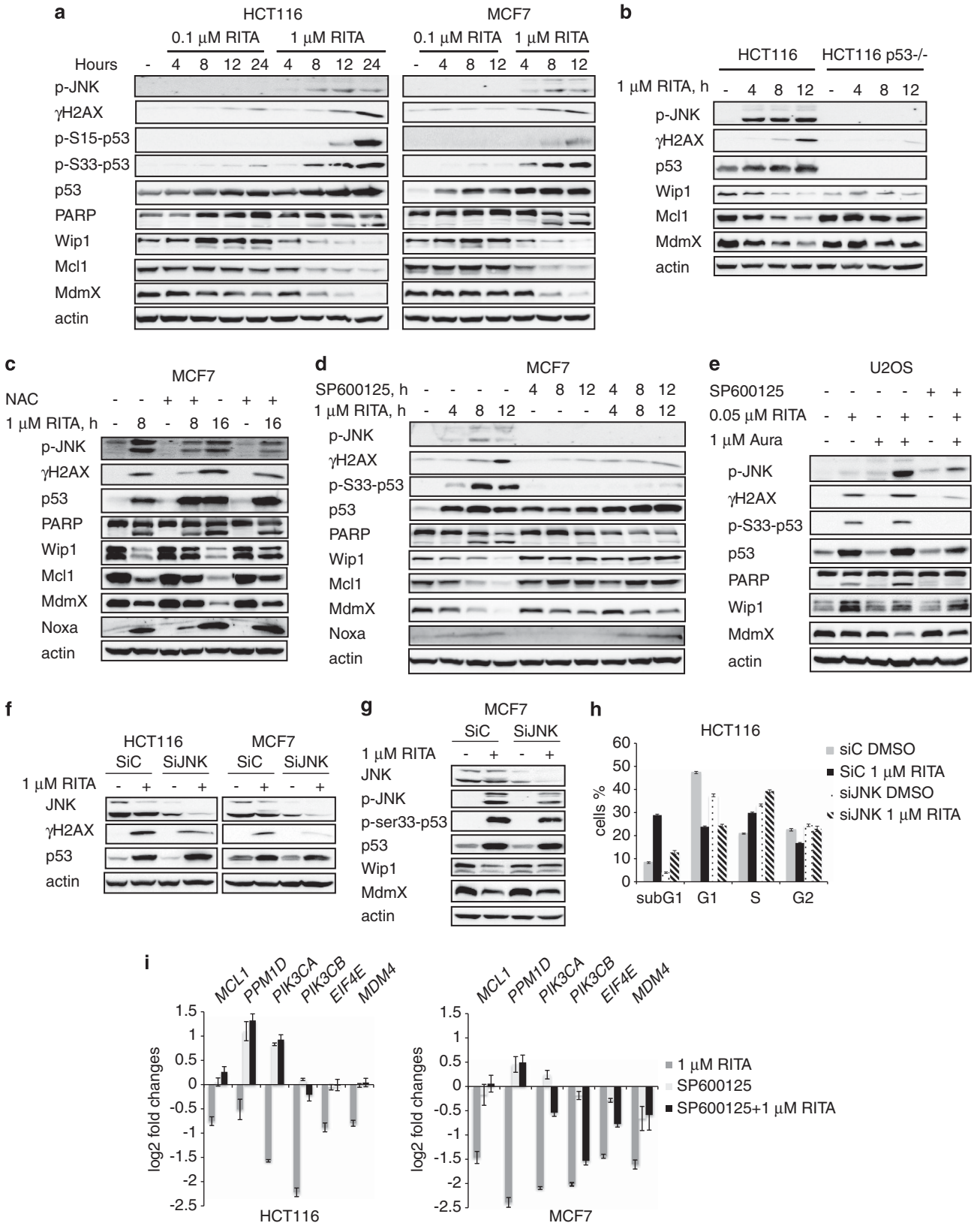
a
HCT116
MCF7
0.1 μM RITA
1 μM RITA
Hours
p-JNK
γH2AX
p-S15-p53
p-S33-p53
p53
PARP
Wip1
Mcl1
MdmX
actin
b
HCT116
HCT116 p53-/-
1 μM RITA, h
c
MCF7
NAC
1 μM RITA, h
Noxa
d
SP600125, h
e
U2OS
SP600125
0.05 μM RITA
1 μM Aura
f
SiC
SiJNK
JNK
g
1 μM RITA
p-ser33-p53
h
HCT116
cells %
siC DMSO
SiC 1 μM RITA
siJNK DMSO
siJNK 1 μM RITA
subG1
G1
S
G2
i
MCL1
PPM1D
PIK3CA
PIK3CB
EIF4E
MDM4
log2 fold changes
1 μM RITA
SP600125
SP600125+1 μM RITA
HCT116
MCF7

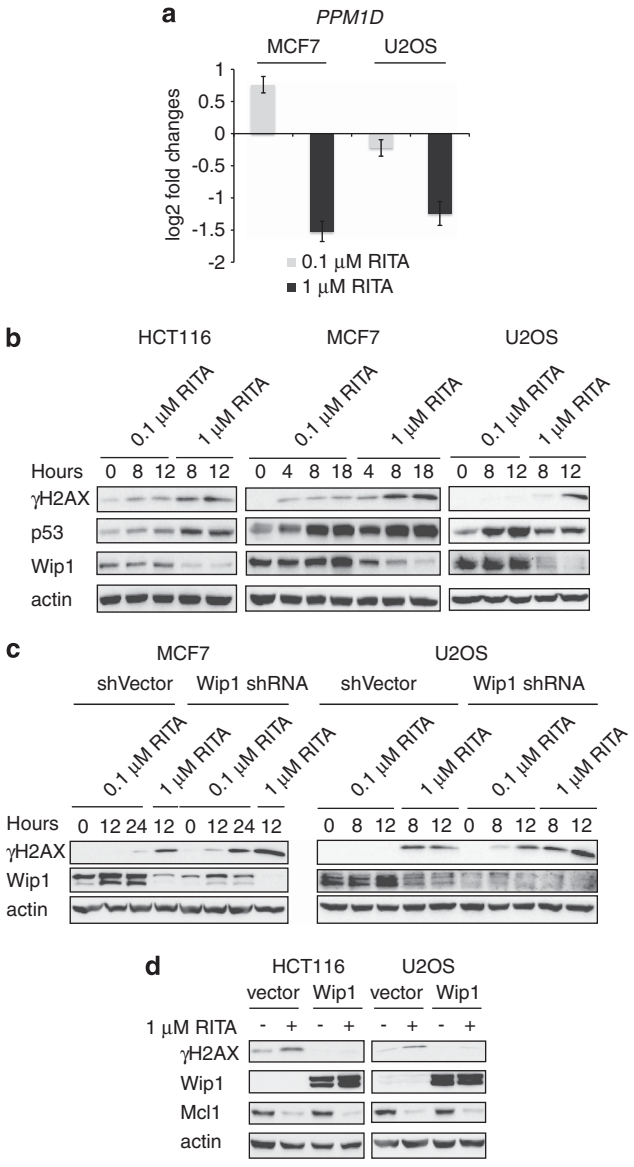

Figure 5 Inhibition of Wip1 promotes the induction of γH2AX upon RITA treatment. (**a**) Wip1 mRNA was repressed after 8 h treatment with 1 μM RITA, but not 0.1 μM RITA, as assessed by qPCR (mean ± S.E.M., $n=3$). (**b**) Down-regulation of Wip1 protein level correlated with the induction of γH2AX upon RITA treatment as analyzed by immunoblotting. (**c**) MCF7 and U2OS cells stably transfected with empty vector shRNA or Wip1 shRNA were treated with 0.1 and 1 μM RITA for indicated periods and γH2AX was assessed as in (**b**). (**d**) HCT116 and U2OS cells transfected with either empty vector or FLAG-Wip1 were treated with 1 μM RITA for indicated times. Proteins were detected by western blotting

S6E and F). We observed a prominent induction of cell death associated with the increase of γH2AX, p53 and decrease of MdmX in the Wip1-silenced cells upon Aura treatment (Supplementary Figures S6C and D). Induction of cell death by Aura in Wip1-depleted cells was comparable with the extent of apoptosis upon Nut/Aura combination, which underscores the crucial role of Wip1.

Taken together, our data demonstrate that the inhibition of Wip1 significantly contributes to the synthetic lethal effects upon p53 activation and TrxR inhibition.

Discussion

Elucidation of the molecular mechanisms governing the cellular responses elicited by p53 is still a challenge in the p53 field, limiting the effective harnessing of p53 activity for cancer treatment.[5] Our present study revealed the crucial role of ROS and activated JNK in p53's proapoptotic function in cancer cells upon pharmacological activation of p53. Further, we elucidated the JNK-mediated mechanisms that play a role in this process and identified a set of key factors downstream of p53 affected by JNK that confer cell death outcome.

Our previous study established that the inhibition of anti-apoptotic factor Mcl1, as well as catalytic subunits of PI3 kinase, translational factor eIF4E and p53 inhibitor MdmX, all well-known oncogenes and a high-priority anti-cancer targets,[37–40] is crucial for the robust apoptosis induction by p53.[15] However, it remained unclear which factors control the inhibition of survival genes by p53. Here, we demonstrated that the ablation of this set of oncogenes by p53 is JNK-dependent.

Despite the extensive efforts, we still have much to learn about the molecular mechanisms of p53-mediated transcriptional repression.[36] p21 has been implicated in the p53-mediated repression of a number of genes.[36] However, p21 is depleted upon p53 activation by RITA, which contributes to the induction of apoptosis,[14] ruling out the possibility that the observed transcriptional repression is p21-dependent.

p53 might have a direct role in the transcriptional repression of several oncogenes, including *EIF4E*, *PPM1D* and *MDM4*, as evidenced by p53 binding to its consensus motif within a short distance from the transcriptional starting site of these genes (Supplementary Table S2), identified by us using p53 chromatin immunoprecipitation followed by deep sequencing (ChIP-seq) described in Nikulenkov *et al*.[7] The binding of p53 to *MYC* and *MCL1* promoters we have previously described.[15,31] However, we cannot rule out an indirect effect

Figure 4 ROS-mediated activation of JNK contributes to the p53-mediated apoptosis, DDR and transcriptional repression of oncogenes. (**a**) Dose-dependent induction of p-JNK, p-Ser33-p53, p-Ser15-p53, γH2AX, PARP cleavage and inhibition of Wip1, Mcl1 and MdmX by RITA as assessed by western blotting. (**b**) HCT116 and HCT116 p53 −/− cells were treated with 1 μM RITA; analyzed as in (**a**). (**c**) Pretreatment with NAC for 6 h prevented the induction of p-JNK, γH2AX, PARP cleavage and inhibition of Wip1, Mcl1 and MdmX by RITA as analyzed by immunoblotting. (**d**) JNK inhibitor SP600125 prevented the induction of p-JNK, p-Ser33-p53, γH2AX, PARP cleavage and inhibition of Wip1, Mcl1 and MdmX by RITA, as assessed by western blotting. (**e**) SP600125 blocked the induction of p-JNK, p-Ser33-p53, γH2AX, PARP cleavage and inhibition of MdmX and Wip1 by combination treatment with 0.05 μM RITA and 1 μM Aura for 24 h, as assessed by western blotting.(**f**, **g**) Depletion of JNK by siRNA prevented the induction of γH2AX (**f**), p-Ser33-p53 and inhibition of Wip1 and MdmX (**g**), analyzed by immunoblotting. (**h**) Inhibition of JNK by siRNA prevented apoptosis induction by RITA, as measured by FACS of PI-stained cells. (**i**) SP600125 blocked the repression of *MCL1, PPM1D, PIK3CA, PIK3CB, EIF4E and MDM4* (MdmX) mRNA upon RITA treatment as assessed by qPCR (mean ± S.E.M., $n=3$) in HCT116 (12 h treatment) and MCF7 (8 h treatment) cells

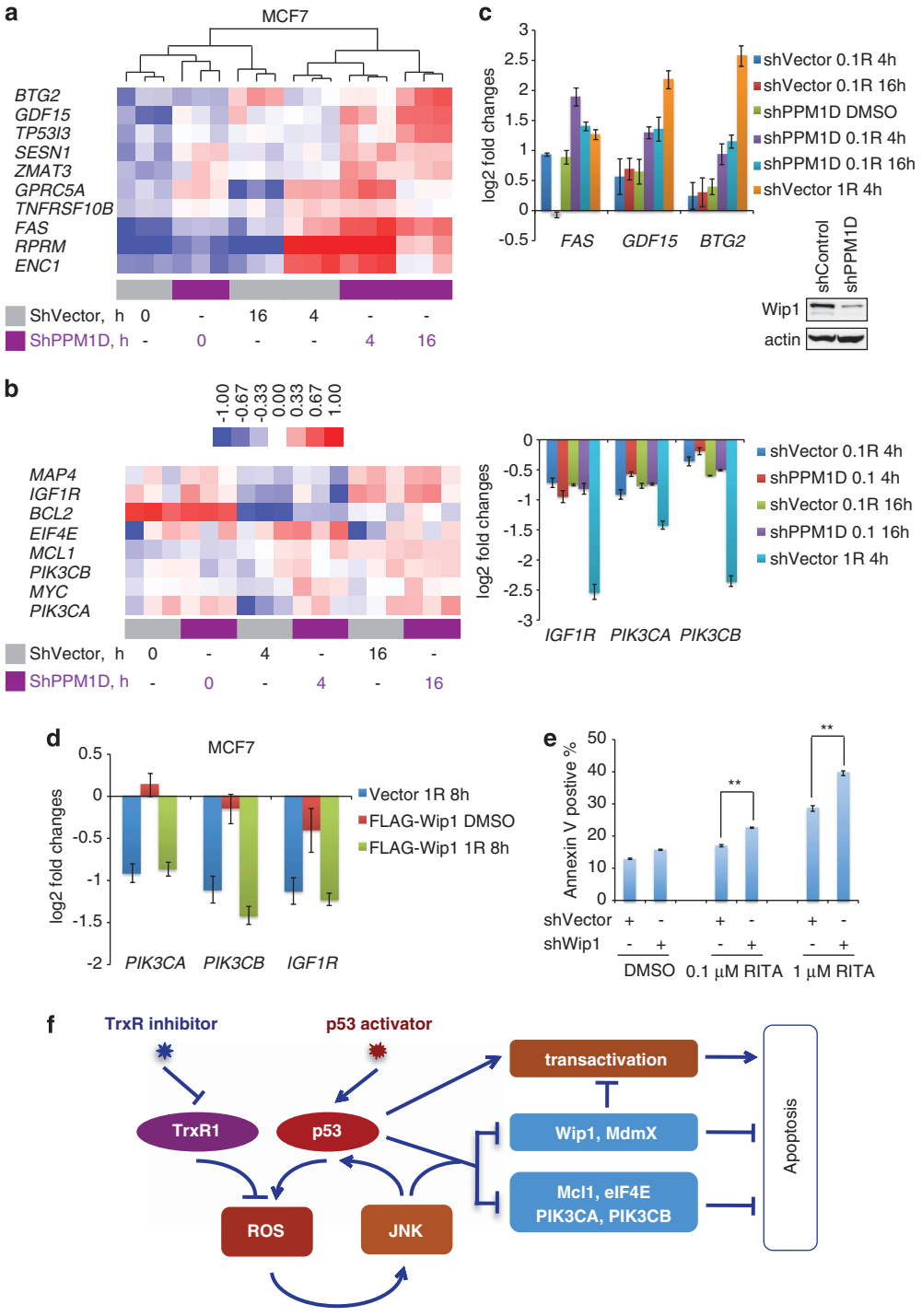

Figure 6 Depletion of Wip1 confers a sustained transcriptional activation of p53 target genes, but does not facilitate transrepression. (**a** and **b**) Microarray analysis of MCF7 cells with (indicated in violet) or without (indicated in gray) Wip1 depletion by shRNA, treated with 0.1 μM RITA or DMSO for indicated time points revealed that p53-mediated transactivation was enhanced by Wip1 silencing. (**c**) Wip1 downregulation led to the increased induction of p53-activated genes (upper panel) but did not augment the repression of pro-survival genes by p53 (lower panel) upon low dose of RITA as analyzed by qPCR (mean ± S.E.M., $n=3$). Insert demonstrates the efficiency of Wip1 depletion, as assessed by immunoblotting. (**d**) MCF7 cells transfected with either empty vector or FLAG-Wip1 were treated with 1 μM RITA or DMSO for 8 h and mRNA levels of *PIK3CA*, *PIK3CB* and *IGF-1R* were assessed by qPCR (mean ± S.E.M., $n=3$). (**e**) MCF7 cells stably transfected with shWip1 or control shVector were treated with 0.1 and 1 μM RITA or DMSO for 24 h, and cells were stained with Annexin V followed by FACS analysis (mean ± S.E.M., $n=3$, $^*P<0.05$, $^{**}P<0.01$, by two-tailed *t*-test). (**f**) Model of the synthetic lethality upon activation of p53 and inhibition of TrxR. Inhibition of TrxR lead to the accumulation of ROS and activation of JNK, facilitating p53 function upon its release from Mdm2. In turn, activated p53 induces pro-oxidant genes, which increases the level of ROS, further activating JNK, and thus, p53. Activated JNK converts p53 to an inhibitor of Wip1 and MdmX, therefore amplifying p53 activity. Transcriptional repression of Mcl1, eIF4E and PI3K abolishes survival signaling, contributing to apoptosis induction. Thus, the dual targeting of p53 and TrxR (i.e., by RITA) leads to the robust apoptosis

of p53 that might be attributed to the p53-regulated microRNAs or other p53-upregulated factors.

We have previously found that p53-activated gene *PPM1D*, whose product Wip1 inhibits p53 signaling,[32] is repressed upon RITA.[35] However, the mechanism of this intriguing phenomenon has not been identified. Our present study implicates JNK as a crucial factor that can convert p53 from a transactivator to a repressor of Wip1.

Based on these results, we suggest a model illustrating how pharmacological release of p53 from the Mdm2 complex, combined with the inhibition of TrxR, results in the excessive accumulation of ROS that leads to further p53 activation by JNK (Figure 6f). In turn, active p53 induces pro-oxidant genes, such as PUMA and PIGs, increasing ROS and further feeding activating signals to JNK and thus, itself. p-JNK converts p53 to an efficient inhibitor of pro-survival oncogenes Mcl1, eIF4E and PI3 kinase, which contributes to apoptosis induction. Further, two p53's own inhibitors, Wip1 and MdmX, are repressed in the p-JNK-dependent manner, which amplifies p53 activation. Establishment of the JNK-p53 positive feedback loop and the inhibition of p53-Wip1 negative feedback loop result in the enhanced and sustained p53 activation. This produces a robust apoptotic outcome, leading to the effective elimination of cancer cells.

Our study also indicates that the induction of ROS might be the cause of the previously observed DNA–DNA and DNA–protein cross-links upon RITA treatment.[19]

Molecular pathways by which reconstituted p53 becomes proapoptotic selectively in malignant tumors are a subject of debate.[2,3,41–43] Reinstatement of p53 efficiently eliminates advanced lung carcinoma cells whereas leaving early lesions unperturbed. This is due to the amplified stress-activated MAPK signaling in advanced lesions, which engages the MDM2 inhibitor p19ARF (p14ARF in humans), in turn activating p53.[2,3] Notably, another *in vivo* study has shown that JNK is required for p53 induction upon oncogene activation.[43]

Our data suggest that elevated ROS in malignant tumors might provide an activating signal to p53 via JNK leading to the enhanced and sustained p53 activity. It is tempting to speculate that this may constitute a basis for the selective elimination of advanced cancers by the reinstated p53, observed in mouse models.[2,3] The relative contribution of the ROS/MAPK pathway in oncogenic signaling and preferential suppression of malignant tumors by p53 is an interesting subject for future studies.

Our results demonstrating that pharmacological activation of p53 in combination with TrxR inhibition and ROS induction confers synthetic lethality could be an important consideration for the clinical application of p53-reactivating drugs. Indeed, we showed that growth arrest/senescence by Nut, which is now being tested in clinic, could be converted to apoptosis upon the low dose of TrxR inhibitor Aura. Furthermore, Aura is an FDA approved drug for the treatment of rheumatoid arthritis; therefore, its repositioning for cancer therapy through the combination strategy as shown in this study will save the time and the cost for developing more effective cancer treatment approaches.

One of the important biochemical differences between normal and cancer cells is a decreased capability of cancer cells to buffer high ROS levels. Our study suggests that dual targeting of p53 and the cellular antioxidant system might allow to maximally exploit the p53-mediated tumor suppression as a therapeutic strategy.

Materials and Methods

Cell culture. Colon carcinoma cell lines HCT116 and HCT116 TP53 $-/-$ were kindly provided by B. Vogelstein, John Hopkins University, USA. p14ARF negative HCT116, HCT116 TP53 $-/-$, breast carcinoma MCF7, osteosarcoma U2OS cells were grown under standard conditions; mammary epithelial cell line MCF10A and 184A1 were obtained from Serhiy Souchelnytskyi, Karolinska Institutet. MCF10A cells were kept in medium containing 50% of MEBM (Clonetics, Basel, Switzerland), 50% of Nutrient Mixture F-12 HAM (Sigma, St. Louis, MO, USA) and 5% horse serum supplemented with MEGM SingleQuot (Clonetics); 184A1 cells were kept in MEGM complete medium supplemented with 5% horse serum.

Plasmids, shRNA and siRNA. Plasmids encoding FLAG-Wip1 and shRNA for Wip1 were kindly provided by René H. Medema, Utrecht, Netherlands. ATM and p53 siRNA were from Santa Cruz Biotechnology (Dallas, TX, USA). Custom siRNA targeting both JNK1 and JNK2[44] was synthesized by Thermo Scientific Dharmacom (Waltham, MA, USA). Plasmid transfection was performed using Lipofectamine 2000 (Invitrogen, Carlsbad, CA, USA) and siRNA was transfected using HiPerFect (Qiagen, Hilden, Germany) according to the manufacturer's instructions.

Drug treatments. RITA was obtained from the National Cancer Institute (NCI). Nut and caffeine from Calbiochem (Billerica, MA, USA) were used at 10 μM and 4 mM, respectively. Resveratrol (BIOMOL International, Farmingdale, NY, USA) was used at 1 μM. Pifithrin-α, SP600125, neocarzinostatin, cisplatin (CDDP), H_2O_2 and NAC (all from Sigma) were used at 10 μM, 40 μM, 200 ng/ml, 50 μM, 400 μM and 5 mM, respectively. Pan-caspase inhibitor Z-VAD-FMK (R&D Systems, Minneapolis, MN, USA) and KU55933 (Tocris Bioscience, Bristol, UK) were used at 10 μM. NDGA, a kind gift from O. Rådmark and Doxorubicin from B. Zhivitovsky, (both from Karolinska Institutet) were used at 10 and 2 μM, respectively.

Molecular and cell biology assays. Western blotting was performed according to a standard procedure. The following antibodies were used: anti-p53 (DO-1), PARP-1/2, Mcl1, c-Myc, phospho-p53 (Ser15), phospho-p53 (Ser33), phospho-JNK (Cell Signaling, Danvers, MA, USA), phospho-histone H2AX (Ser139) (Millipore, Billerica, MA, USA), ATM (Abcam, Cambridge, UK), Wip1 (Bethyl Laboratories, Montgomery, TX, USA), Noxa, Puma (Calbiochem), β-actin (Sigma). After transfer membranes were cut to detect several proteins on the same membrane; in Figure 4 and Supplementary Figure S5, the proteins were detected in the following order: (1) Wip1, p-JNK (30 min exposure), γH2AX; (2) MdmX, p-S15-p53, actin, Puma; (3) PARP, p-S33-p53, Mcl1, Noxa; (4) p53.

Alkaline comet assay, FACS analysis of propidium iodide (PI)-stained cells and qPCR were performed as described Imreh *et al.*[45] and Enge *et al.*[14] FACS analysis of FITC-Annexin V and PI (from BD Biosciences, San Jose, CA, USA) double-stained cells was performed according to the manufacturer's protocols. Detection of activated caspases by FAM-FLICA Poly-Caspase Detection Kit from Immuno-Chemistry Technologies (Bloomington, MN, USA) was performed using FACS according to the manufacture's protocol.

Primers are described in Supplementary Table S3.

ROS measurement. ROS were measured as in Hedstrom *et al.*[21] Briefly, after treatment with different compounds, cells were washed once with serum-free medium and incubated with 10 μM 2′,7′-dichlorodihydrofluorescein diacetate (DCF-DA) in serum-free medium for half an hour under standard conditions; then cells were washed twice with PBS, trypsinized, harvested and washed another two times with PBS. The samples were sorted on Becton Dickinson FCAScan using FL1-H channel, and analyzed by CellQuest (San Jose, CA, USA) software 4.0.2.

Microarray analysis. Systematic clustering of gene expression data was performed with CRC clustering method, implemented in geneXplain platform (www.genexplain.com).[46] When applied to 2000 10-point profiles with the largest

fold change, the method gives about 10 high quality clusters with more than 40 profiles in them, and with the gene lists of the clusters enriched in GO terms at *P*-value < 0.002. To compare gene expression profiles under different treatments, we plot the mean expression profile of the clustered genes in one case and the mean profile of the same (not clustered) genes in other cases. This allowed detecting of conserved and variable features.

p53 ChIP-seq. The detailed description of p53 ChIP-seq experiment is provided in Nikulenkov *et al.*[7] The analysis of p53 binding to inhibited genes was performed as described in Zawacka-Pankau *et al.*[31]

***In vitro* assay of TrxR1 activity.** In this inhibition analysis, 50 nM wild-type TrxR1 (24.0 U/mg) was reduced by 150 μM NADPH in TE buffer (pH 7.5) and then RITA at defined concentration ranging from 0.1 to 200 μM was incubated with the reduced enzyme in the dark at room temperature for 60 min. DMSO instead of RITA was used as control. Small aliquots of RITA-inhibited enzyme were taken out at 60-min time point for measuring the DTNB reduction activity and the NADPH-reduced enzyme was used as control. After TrxR1 activity was inhibited, 500 μl RITA-inhibited TrxR1 (50 nM) was applied onto TE-equilibrated NAP-5 column (GE Healthcare Life Sciences, Uppsala, Sweden) and then eluted with 1 ml TE buffer. TrxR1 activities using DTNB (2.5 mM), human Trx1 (20 μM) and juglone (50 μM) as substrates were measured after desalting. DTNB reduction was measured at 412 nm (extinction coefficient of 13 600 M/cm) by adding the desalted enzyme respectively into the DTNB reaction mixture (200 μl) containing 2.5 mM DTNB, 300 μM NADPH and 4.5 nM enzyme in TE buffer (pH 7.5). Trx-coupled insulin assay was performed by measuring the NADPH consumption at 340 nm (extinction coefficient of 6220 M/cm) and reaction system contains 20 μM human Trx1, 160 μM insulin, 300 μM NADPH and 9 nM enzyme in TE buffer (pH 7.5). The NADPH oxidase activity was monitored as the decrease at 340 nm (extinction coefficient of 6220 M/cm) for 60 min. The reaction system (200 μl) contains 50 μM juglone, 200 μM NADPH and 4.5 nM enzyme in TE buffer (pH 7.5). Enzymatic reactions and measurements were performed with 10-sec time interval reads at 25 °C using a VersaMax microplate reader (Molecular Devices, Sunnyvale, CA, USA), with the reaction mixtures without enzyme serving as reference. Activity measurements were performed in triplicate and analyzed with the Prism 5 software (GraphPad, La Jolla, CA, USA).

Conflict of Interest

The authors declare no conflict of interest.

Acknowledgements. This study was supported by the Swedish Cancer Society, the Swedish Research Council, Ragnar Söderberg Foundation, and the Karolinska Institutet/Stockholm County Council (ACT! Theme center) and partially supported by the FP7 grants: SysCol (no. 258236) and MIMOMICS (no. 305280). JZ-P would like to acknowledge the Award for Young Talented Investigators and IUVENTUS PLUS 0635/IP1/2011/71 from Polish Ministry of Science and Higher Education. We are greatly indebted to B Zhivotovsky and G Imreh for their help with comet assay and to all our colleagues who shared valuable reagents and cell lines with us.

1. Selivanova G. Therapeutic targeting of p53 by small molecules. *Semin Cancer Biol* 2010; **20**: 46–56.
2. Junttila MR, Karnezis AN, Garcia D, Madriles F, Kortlever RM, Rostker F *et al.* Selective activation of p53-mediated tumour suppression in high-grade tumours. *Nature* 2010; **468**: 567–571.
3. Feldser DM, Kostova KK, Winslow MM, Taylor SE, Cashman C, Whittaker CA *et al.* Stage-specific sensitivity to p53 restoration during lung cancer progression. *Nature* 2010; **468**: 572–575.
4. Xue W, Zender L, Miething C, Dickins RA, Hernando E, Krizhanovsky V *et al.* Senescence and tumour clearance is triggered by p53 restoration in murine liver carcinomas. *Nature* 2007; **445**: 656–660.
5. Vousden KH, Prives C. Blinded by the light: the growing complexity of p53. *Cell* 2009; **137**: 413–431.
6. Jackson JG, Pant V, Li Q, Chang LL, Quintas-Cardama A, Garza D *et al.* p53-mediated senescence impairs the apoptotic response to chemotherapy and clinical outcome in breast cancer. *Cancer Cell* 2012; **21**: 793–806.
7. Nikulenkov F, Spinnler C, Li H, Tonelli C, Shi Y, Turunen M *et al.* Insights into p53 transcriptional function via genome-wide chromatin occupancy and gene expression analysis. *Cell Death Differ* 2012; **19**: 1992–2002.
8. Haigis KM, Sweet-Cordero A. New insights into oncogenic stress. *Nat Genet* 2011; **43**: 177–178.
9. Trachootham D, Alexandre J, Huang P. Targeting cancer cells by ROS-mediated mechanisms: a radical therapeutic approach? *Nat Rev Drug Discov* 2009; **8**: 579–591.
10. Arner ES, Holmgren A. The thioredoxin system in cancer. *Semin Cancer Biol* 2006; **16**: 420–426.
11. Hatfield DL, Yoo MH, Carlson BA, Gladyshev VN. Selenoproteins that function in cancer prevention and promotion. *Biochim Biophys Acta* 2009; **1790**: 1541–1545.
12. Urig S, Becker K. On the potential of thioredoxin reductase inhibitors for cancer therapy. *Semin Cancer Biol* 2006; **16**: 452–465.
13. Brown CJ, Lain S, Verma CS, Fersht AR, Lane DP. Awakening guardian angels: drugging the p53 pathway. *Nat Rev Cancer* 2009; **9**: 862–873.
14. Enge M, Bao W, Hedstrom E, Jackson SP, Moumen A, Selivanova G. MDM2-dependent downregulation of p21 and hnRNP K provides a switch between apoptosis and growth arrest induced by pharmacologically activated p53. *Cancer Cell* 2009; **15**: 171–183.
15. Grinkevich VV, Nikulenkov F, Shi Y, Enge M, Bao W, Maljukova A *et al.* Ablation of key oncogenic pathways by RITA-reactivated p53 is required for efficient apoptosis. *Cancer Cell* 2009; **15**: 441–453.
16. Ahmed A, Yang J, Maya-Mendoza A, Jackson DA, Ashcroft M. Pharmacological activation of a novel p53-dependent S-phase checkpoint involving CHK-1. *Cell Death Dis* 2011; **2**: e160.
17. Secchiero P, Bosco R, Celeghini C, Zauli G. Recent advances in the therapeutic perspectives of Nutlin-3. *Curr Pharm Des* 2011; **17**: 569–577.
18. Komarov PG, Komarova EA, Kondratov RV, Christov-Tselkov K, Coon JS, Chernov MV *et al.* A chemical inhibitor of p53 that protects mice from the side effects of cancer therapy. *Science* 1999; **285**: 1733–1737.
19. Nieves-Neira W, Rivera MI, Kohlhagen G, Hursey ML, Pourquier P, Sausville EA *et al.* DNA protein cross-links produced by NSC 652287, a novel thiophene derivative active against human renal cancer cells. *Mol Pharmacol* 1999; **56**: 478–484.
20. Sedelnikova OA, Redon CE, Dickey JS, Nakamura AJ, Georgakilas AG, Bonner WM. Role of oxidatively induced DNA lesions in human pathogenesis. *Mutat Res* 2010; **704**: 152–159.
21. Hedstrom E, Eriksson S, Zawacka-Pankau J, Arner ES, Selivanova G. p53-dependent inhibition of TrxR1 contributes to the tumor-specific induction of apoptosis by RITA. *Cell Cycle* 2009; **8**: 3576–3583.
22. Anestal K, Arner ES. Rapid induction of cell death by selenium-compromised thioredoxin reductase 1 but not by the fully active enzyme containing selenocysteine. *J Biol Chem* 2003; **278**: 15966–15972.
23. Anestal K, Prast-Nielsen S, Cenas N, Arner ES. Cell death by SecTRAPs: thioredoxin reductase as a prooxidant killer of cells. *PLoS ONE* 2008; **3**: e1846.
24. He X, Andersson G, Lindgren U, Li Y. Resveratrol prevents RANKL-induced osteoclast differentiation of murine osteoclast progenitor RAW 264.7 cells through inhibition of ROS production. *Biochem Biophys Res Commun* 2010; **401**: 356–362.
25. Floriano-Sanchez E, Villanueva C, Medina-Campos ON, Rocha D, Sanchez-Gonzalez DJ, Cardenas-Rodriguez N *et al.* Nordihydroguaiaretic acid is a potent *in vitro* scavenger of peroxynitrite, singlet oxygen, hydroxyl radical, superoxide anion and hypochlorous acid and prevents *in vivo* ozone-induced tyrosine nitration in lungs. *Free Radic Res* 2006; **40**: 523–533.
26. Marzano C, Gandin V, Folda A, Scutari G, Bindoli A, Rigobello MP. Inhibition of thioredoxin reductase by auranofin induces apoptosis in cisplatin-resistant human ovarian cancer cells. *Free Radic Biol Med* 2007; **42**: 872–881.
27. Bragado P, Armesilla A, Silva A, Porras A. Apoptosis by cisplatin requires p53 mediated p38alpha MAPK activation through ROS generation. *Apoptosis* 2007; **12**: 1733–1742.
28. Prast-Nielsen S, Cebula M, Pader I, Arner ES. Noble metal targeting of thioredoxin reductase–covalent complexes with thioredoxin and thioredoxin-related protein of 14 kDa triggered by cisplatin. *Free Radic Biol Med* 2010; **49**: 1765–1778.
29. Seyfried J, Wullner U. Inhibition of thioredoxin reductase induces apoptosis in neuronal cell lines: role of glutathione and the MKK4/JNK pathway. *Biochem Biophys Res Commun* 2007; **359**: 759–764.
30. de Feraudy S, Revet I, Bezrookove V, Feeney L, Cleaver JE. A minority of foci or pan-nuclear apoptotic staining of gammaH2AX in the S phase after UV damage contain DNA double-strand breaks. *Proc Natl Acad Sci USA* 2010; **107**: 6870–6875.
31. Zawacka-Pankau J, Grinkevich VV, Hunten S, Nikulenkov F, Gluch A, Li H *et al.* Inhibition of glycolytic enzymes mediated by pharmacologically activated p53: targeting Warburg effect to fight cancer. *J Biol Chem* 2011; **286**: 41600–41615.
32. Le Guezennec X, Bulavin DV. WIP1 phosphatase at the crossroads of cancer and aging. *Trends Biochem Sci* 2010; **35**: 109–114.
33. Macurek L, Lindqvist A, Voets O, Kool J, Vos HR, Medema RH. Wip1 phosphatase is associated with chromatin and dephosphorylates gammaH2AX to promote checkpoint inhibition. *Oncogene* 2010; **29**: 2281–2291.
34. Moon SH, Lin L, Zhang X, Nguyen TA, Darlington Y, Waldman AS *et al.* Wild-type p53-induced phosphatase 1 dephosphorylates histone variant gamma-H2AX and suppresses DNA double strand break repair. *J Biol Chem* 2010; **285**: 12935–12947.

35. Spinnler C, Hedstrom E, Li H, de Lange J, Nikulenkov F, Teunisse AF *et al.* Abrogation of Wip1 expression by RITA-activated p53 potentiates apoptosis induction *via* activation of ATM and inhibition of HdmX. *Cell Death Differ* 2011; **18**: 1736–1745.
36. Riley T, Sontag E, Chen P, Levine A. Transcriptional control of human p53-regulated genes. *Nat Rev Mol Cell Biol* 2008; **9**: 402–412.
37. Akgul C. Mcl-1 is a potential therapeutic target in multiple types of cancer. *Cell Mol Life Sci* 2009; **66**: 1326–1336.
38. Gustin JP, Cosgrove DP, Park BH. The PIK3CA gene as a mutated target for cancer therapy. *Curr Cancer Drug Targets* 2008; **8**: 733–740.
39. Blagden SP, Willis AE. The biological and therapeutic relevance of mRNA translation in cancer. *Nat Rev Clin Oncol* 2011; **8**: 280–291.
40. Marine JC, Dyer MA, Jochemsen AG. MDMX: from bench to bedside. *J Cell Sci* 2007; **120**(Pt 3): 371–378.
41. Bartkova J, Horejsi Z, Koed K, Kramer A, Tort F, Zieger K *et al.* DNA damage response as a candidate anti-cancer barrier in early human tumorigenesis. *Nature* 2005; **434**: 864–870.
42. Gorgoulis VG, Vassiliou LV, Karakaidos P, Zacharatos P, Kotsinas A, Liloglou T *et al.* Activation of the DNA damage checkpoint and genomic instability in human precancerous lesions. *Nature* 2005; **434**: 907–913.
43. Schramek D, Kotsinas A, Meixner A, Wada T, Elling U, Pospisilik JA *et al.* The stress kinase MKK7 couples oncogenic stress to p53 stability and tumor suppression. *Nat Genet* 2011; **43**: 212–219.
44. Carew JS, Nawrocki ST, Reddy VK, Bush D, Rehg JE, Goodwin A *et al.* The novel polyamine analogue CGC-11093 enhances the antimyeloma activity of bortezomib. *Cancer Res* 2008; **68**: 4783–4790.
45. Imreh G, Norberg HV, Imreh S, Zhivotovsky B. Chromosomal breaks during mitotic catastrophe trigger gammaH2AX-ATM-p53-mediated apoptosis. *J Cell Sci* 2011; **124**(Pt 17): 2951–2963.
46. Qin ZS. Clustering microarray gene expression data using weighted Chinese restaurant process. *Bioinformatics* 2006; **22**: 1988–1997.

Supplementary Information accompanies this paper on Cell Death and Differentiation website (http://www.nature.com/cdd)